ABCM

NATURAL CONVECTION BETWEEN CONCENTRIC ELLIPSES ANALYSIS OF THE LIMITING CASES

Cunha, A. R., Livramento, M. A., Vasconcellos, J. F. and Maliska, C. R.

SINMEC - Computational Fluid Dynamics Laboratory
Mechanical Engineering Department - UFSC
88040-900- Florianópolis - SC- Brazil

SUMMARY - *The natural convection flow between concentric ellipses is analyzed numerically using a boundary-fitted finite volume method. A family of elliptical cavities, using the ratios of ellipses semi-axis and theirs perimeters, is generated. Interesting flow patterns are obtained in the limiting cases, being one of them the appearance of the Bénard cells when part of the cavity resembles the parallel plates configuration.*

INTRODUCTION

Natural convection heat transfer inside cavities has received a great deal of attention due in part to its importance in fundamental and applied science. Numerical works have been done to solve the buoyancy-driven flow on several kinds of geometrically complex enclosures. By large, these works have been focused on the rectangular and cylindrical enclosures. Although to the authors knowledge, the problem here proposed was not yet solved, there is a large number of numerical solutions for non-rectangular geometries. Related to elliptical cavities very few analysis are registered in the literature. Campo *et alii* (1987) carried out a study about natural convection in a semielliptic cavity using a finite-element algorithm. Schreiber and Singh (1987) analyzed the natural convection between confocal ellipses considering stable and instable stratification. However, the boundary conditions employed up to now do not allow the appearance of the Bénard flow, one of the limiting cases analyzed in this work.

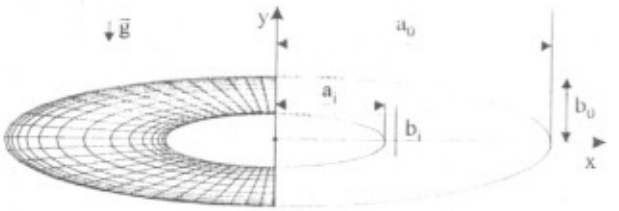

Figure 1 - Elliptical geometry

The present work is based on the numerical solution of the two-dimensional form of the Navier-Stokes and energy equations with constant properties. Viscous dissipation and compression work are neglected. Attention will be concentrated upon buoyancy-driven cavity flow on elliptic geometry using boundary-fitted coordinates.

A finite volume method using non-orthogonal grids with co-located variables was used to formulate the algebraic equation approximations. The difficulty associated with the use of co-located variables was removed using the approximation of the pressure gradients proposed by Peric *et alii* (1988), with the improvements presented in Marchi and Maliska (1994).

Computations were performed for Rayleigh number, Ra_L, in the range from 1×10^3 to 1×10^7, with the perimeter ratio, Per_i / Per_o, ranging from 0.2 to 0.6 and the ratio b_o / a_o ranging from 1 / 4 to 4 / 1.

Of key interest in this work is to capture the Bénard cells when the configuration resembles the problem of parallel plates heated from below.

The following sections outline the governing equations, the numerical scheme, results and discussions.

FORMULATION OF THE PROBLEM

The one-half enclosure model is presented in Fig. 1. The fluid is treated as Newtonian and incompressible. The dependence of the density on temperature is introduced through the Boussinesq approximation:

$$\rho = \rho_c\left[1 + \beta\left(T - T_{ref}\right)\right] \tag{1}$$

where $T_{ref} = \left(T_o + T_i\right)/2$ is the average temperature, ρ the density, ρ_c the reference density, β the coefficient of volumetric expansion, T_o the temperature of the outer wall and T_i the temperature of the inner wall. The enclosure is initially occupied by motionless fluid. The initial fluid temperature is uniform and equal to T_{ref}. T_i is always greater than T_o

The equations governing are:

$$\frac{\partial u}{\partial x} + \frac{\partial v}{\partial y} = 0 \tag{2}$$

$$\frac{\partial}{\partial x}\left[\rho\, u\, u - \mu\,\frac{\partial u}{\partial x}\right] + \frac{\partial}{\partial y}\left[\rho\, u\, v - \mu\,\frac{\partial u}{\partial y}\right] = -\frac{\partial p}{\partial x} \tag{3}$$

$$\frac{\partial}{\partial x}\left[\rho\, u\, v - \mu\,\frac{\partial v}{\partial x}\right] + \frac{\partial}{\partial y}\left[\rho\, v\, v - \mu\,\frac{\partial v}{\partial y}\right] = -\frac{\partial p}{\partial y} + \rho\, g\, \beta\left(T - T_{ref}\right) \tag{4}$$

$$\frac{\partial}{\partial x}\left[\rho u T - \frac{k}{c_p}\frac{\partial T}{\partial x}\right]+\frac{\partial}{\partial y}\left[\rho v T - \frac{k}{c_p}\frac{\partial T}{\partial y}\right]=0 \qquad (5)$$

Considering that two-dimensional flow exists, due to symmetry, the equations are solved in half of the region.

The boundary conditions are as follows:

Inner surface:

$$u = v = 0 \quad \text{and} \quad T = T_i \qquad (6)$$

Outer surface:

$$u = v = 0 \quad \text{and} \quad T = T_o \qquad (7)$$

Symmetry lines:

$$u = \frac{\partial v}{\partial \vec{n}} = \frac{\partial T}{\partial \vec{n}} = 0 \qquad (8)$$

where $\vec{n}$ is the normal with respect to the boundary.

The Rayleigh number is defined as:

$$Ra_L = \frac{\rho g \beta \left(T_i - T_o\right) L^3}{\nu^2} Pr \qquad (9)$$

where $L = \left(Per_o - Per_i\right)/2\pi$. Per_i and Per_o are the inner and outer perimeter of the geometry. In this work, the rate b_o / a_o is always equal to the rate b_i / a_i (see Fig. 1).

The equation written for a general coordinate system (ξ, η) for a generic scalar ϕ is (Maliska, 1995):

$$\frac{\partial}{\partial \xi}(\rho U \phi)+\frac{\partial}{\partial \eta}(\rho V \phi)=\frac{\partial}{\partial \xi}\left(c_1 \Gamma \frac{\partial \phi}{\partial \xi}\right)+\frac{\partial}{\partial \xi}\left(c_2 \Gamma \frac{\partial \phi}{\partial \eta}\right)+ \frac{\partial}{\partial \eta}\left(c_2 \Gamma \frac{\partial \phi}{\partial \xi}\right)+\frac{\partial}{\partial \eta}\left(c_4 \Gamma \frac{\partial \phi}{\partial \eta}\right)+ S^\phi - P^\phi \qquad (10)$$

where

$$\begin{aligned} U &= u\, y_\eta - v\, x_\eta \\ V &= v\, y_\xi - u\, x_\xi \\ J &= \left(x_\xi\, y_\eta - x_\eta\, y_\xi\right)^{-1} \\ c_1 &= J\left(x_\eta\, x_\eta + y_\eta\, y_\eta\right) \\ c_2 &= -J\left(x_\xi\, x_\eta + y_\xi\, y_\eta\right) \\ c_4 &= J\left(x_\xi\, x_\xi + y_\xi\, y_\xi\right) \end{aligned} \qquad (11)$$

The ϕ variable represents the mass conservation equation, the two cartesian velocity components u and v in the x and y directions, respectively, and T the temperature. The values of Γ, S^ϕ, P^ϕ are summarized in Table 1.

Table 1 - Values of Γ, S^ϕ and P^ϕ

ϕ	Γ	S^ϕ	P^ϕ
1	0	0	0
u	μ	0	$y_\eta \frac{\partial P^*}{\partial \xi} - y_\xi \frac{\partial P^*}{\partial \eta}$
v	μ	$\rho g \beta\left(T - T_{ref}\right)$	$x_\xi \frac{\partial P^*}{\partial \eta} - x_\eta \frac{\partial P^*}{\partial \xi}$
T	$\frac{k}{c_p}$	0	0

DISCRETIZED EQUATIONS

To obtain the discretized equations using the finite-volume concept, Eq. (10) is integrated over the regular elemental volume in the (ξ, η) domain, see Fig. 2.

The value of ϕ and its derivatives at the control volume interfaces are evaluated, as a function of nodal points, using the WUDS scheme (Raithby and Torrance, 1974).

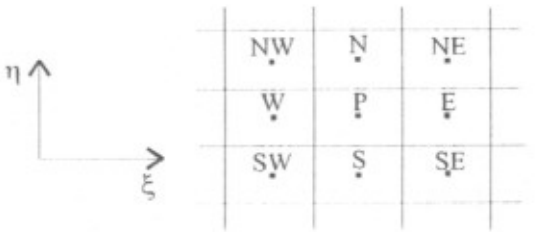

Figure 2 - Computational domain

Integration of the Eq. (10) in space results in:

$$\begin{aligned} M_e\phi_e - M_w\phi_w + M_n\phi_n - M_s\phi_s = -L\left[\hat{P}^\phi\right]_P \Delta V - \\ L\left[\hat{S}^\phi\right]_P \Delta V + \left[D_1\frac{\partial\phi}{\partial\xi} + D_2\frac{\partial\phi}{\partial\eta}\right]_e - \left[D_1\frac{\partial\phi}{\partial\xi} + D_2\frac{\partial\phi}{\partial\eta}\right]_w + \\ \left[D_3\frac{\partial\phi}{\partial\xi} + D_4\frac{\partial\phi}{\partial\eta}\right]_n - \left[D_3\frac{\partial\phi}{\partial\xi} + D_4\frac{\partial\phi}{\partial\eta}\right]_s \end{aligned} \qquad (12)$$

where M_e and D_1, for example, are given by

$$\begin{aligned} M_e &= (\rho U)_e \Delta\eta \\ D_1 &= \Gamma^\phi c_2 J \Delta\eta \end{aligned} \qquad (13)$$

and $L[\ ]$ means the numerical approximation of the term inside the brackets.

NUMERICAL SCHEME

The general purpose computer code, SINFLOW, was used to compute these flows. It is a computer program, available at the SINMEC, developed to solve two-dimensional transient laminar problems using the finite volume approach based in a boundary-fitted framework, with a co-located scheme for dependent vari-

ables (u, v, P and T), as described in Marchi and Maliska (1994). It uses the SIMPLEC method proposed by Van Doormaal and Raithby (1984) for treating the pressure-velocity coupling.

The results shown in this work were performed on a 30 x 60 grid in the radial and circumferential direction, respectively. Explanatory study on coarser and finer grids were performed to provide guidance for choosing the best grid. The grid lines were more closely packed near the boundaries, as shown in the left side of the Fig. 1.

The convergence criterion includes the overall energy balance for the cavity as follows

$$\frac{Nu_o - Nu_i}{Nu_o} \leq 10^{-5} \qquad (14)$$

where Nu_o and Nu_i are proportional to the heat transport across the outer an inner surface, respectively. This convergence criterion assures that the energy conservation equation is being satisfied according to the specific tolerance.

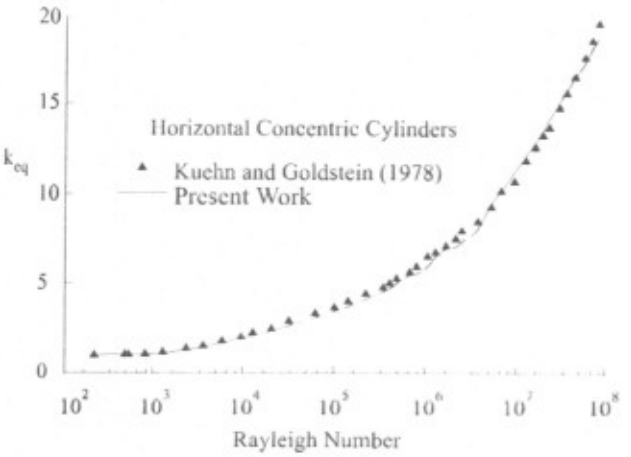

Figure 3 - Horizontal concentric cylinder. Comparison with experimental data

All computation were performed on an SUN SPARK 10 computer with two scalar processors.

Eq. (12), after using the interpolation functions, written in compact form is,

$$a_P \phi_P = \sum a_{nb} \phi_{nb} + \left(L\left[S^{\phi}\right] - L\left[P^{\phi}\right] \right) \Delta V_P \qquad (15)$$

where "a" is the coefficients in the linear equations and L[ ] means the numerical approximation of the source term in the equation for ϕ. To solve the four systems of algebraic equation are solved by an ADI procedure as described in Silva *et alii* (1991). To obtain the values of u, v, T and p the following procedure was used (Maliska, 1995):

1) The initial condition is assigned to all volumes in domain.

2) Calculate the coefficients and source terms for u and v. Solve the corresponding linear systems.

3) Calculate the coefficients and solve the pressure correction equation. (SIMPLEC method).

4) The velocities u and v are corrected using the pressure correction calculated in step 3.

5) Solve for temperature.

6) Return to step 2 until the convergence criteria is achieved.

RESULTS AND DISCUSSION

The results are presented using the average heat transfer rate in the form of an equivalent conductivity

$$k_{eq} = \frac{\overline{Nu}}{\overline{Nu}_{cond}} \qquad (16)$$

where $\overline{Nu}$ is the average Nusselt number and $\overline{Nu}_{cond}$ is the Nusselt number for $Ra_L = 0$.

TEST CASE:

This problem precludes any analytical solution, but it is possible to check the numerical model with the available numerical and experimental data. One chooses the experimental results of Kuehn and Goldstein (1978) due to its reliability.

The geometry is a concentric horizontal cylindrical annuli with the ratio $a_i / a_o = 2.6$ and the ratio $b_i / a_i = 1$. Fig. 3 shows the comparison between their experimental data and the model used in this work. The numerical predictions are in very good agreement with the experimental measurements.

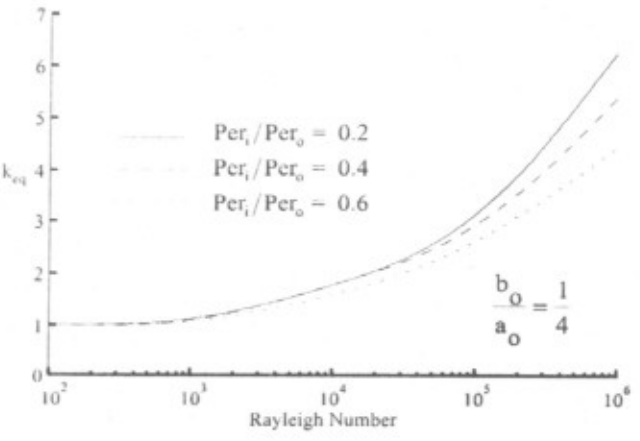

Figure 4 - Influence of the perimeter ratio Per_i / Per_o and Rayleigh Number on the k_{eq}, for $b_o / a_o = 1/4$

ELLIPITIC CAVITIES

Numerical results were obtained for many different elliptical cavities, changing the perimeter ratio and b_o / a_o. As mentioned, one is interested finding the elliptical cavities which presents the Bénard cells.

Fig. 4 shows the behavior of the equivalent conductivity, k_{eq}, with Reynolds number, Ra_L, for a cavity with

$b_o / a_o = 1/4$. Three perimeter ratios were analyzed: 0.2, 0.4 and 0.6. These geometries can be seen in Figs. 7, 8 and 9, respectively.

Table 2 - Nusselt number for pure conduction

Per_i / Per_o	$\overline{Nu}_{cond}$
0.2	1.1986
0.4	2.1513
0.6	3.9152

It can be seen in Fig. 4 that k_{eq} increases when the perimeter ratio decreases. In order to appreciate this behavior it is necessary to compute the Nusselt number for pure conduction, this is, for $Ra_L = 0$. Table 2 shows that when the perimeter ratio increases the heat transfer by conduction also increases, since the two walls get closer and the conduction resistance decreases. Therefore, the decrease in k_{eq} when the perimeter ratio increases is due, mainly, to the rapid growth of Nu_e with the increase in perimeter ratio.

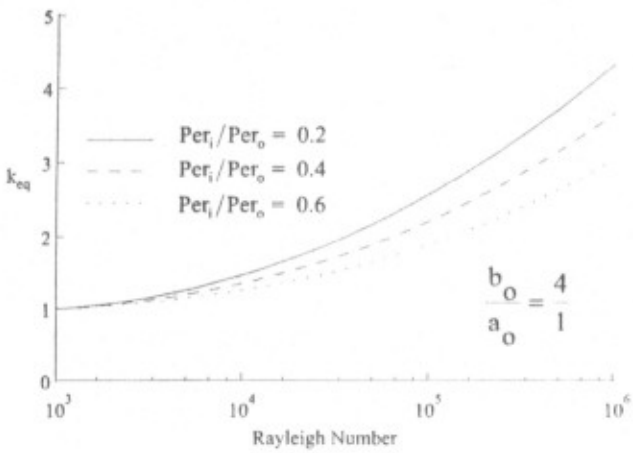

Figure 5 - Influence of the perimeter ratio Per_i / Per_o and Rayleigh Number on the k_{eq}, for $b_o / a_o = 4/1$.

Increasing L one approaches the situation where part of the horizontal internal wall (heated) is parallel to part of the external wall (cooled). This reproduces the well know Bénard problem, were pairs of convective cells arises depending on the size of the cavity.

Fig. 5 shows the behavior of the equivalent conductivity, k_{eq}, with Reynolds number, Ra_L, for a cavity with $b_o / a_o = 4/1$. Three perimeter ratios were analyzed: 0.2, 0.4 and 0.6. Fig. 10 shows two cavities with this b_o / a_o ratio. The behavior showed in Fig. 5 is the same of the Fig. 4. The greater the perimeter ratio is the smaller convective cells are.

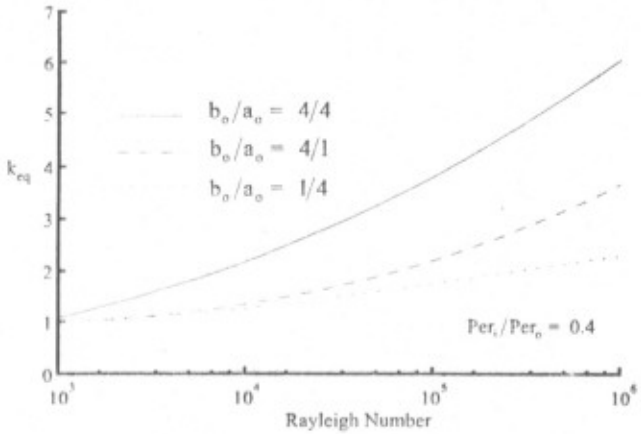

Figure 6 - Influence of the ratio b_o / a_o and Rayleigh Number on the k_{eq} for the perimeter ratio $Per_i / Per_o = 0.4$

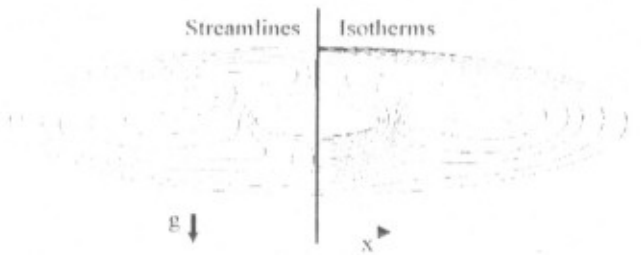

Figure 7 - Streamlines and isotherms for $b_o / a_o = 1/4$, $Per_i / Per_o = 0.2$ and Rayleigh number 10^5.

Fig. 6 shows the influence of the ratio b_o / a_o and Rayleigh number on the k_{eq} for the perimeter ratio $Per_i / Per_o = 0.4$. This figure shows that a cylindrical cavities are better geometries to the heat transport. Convective cells are bigger in this cavities than in the others. It can be seen also that the geometry which presents the Bénard cells ($b_o / a_o = 1/4$) shows smaller k_{eq} then the one with ($b_o / a_o = 4/1$), that is, the vertical cavity. This was also expected since the heat is easier transported by the flow movements of the vertical cavity than by the flow which characterizes the Bénard cells. Recall that for these two geometries heat transfer by conduction is equal, therefore, the difference in k_{eq} is due solely to convection effects.

Two equations approximating the calculated results are as follows:

$$k_{eq_1} = 0.1565 \left(Ra_e\right)^{0.2093} \left(\frac{b_o}{a_o}\right)^{0.0201} \left(d_e\right)^{0.1309} \quad (17)$$

$$k_{eq} = 0.1257 \left(Ra_e\right)^{0.2303} \left(\frac{b_o}{a_o}\right)^{0.0591} \left(d_e\right)^{0.1316} \quad (18)$$

where Ra_e is the Rayleigh number defined in equation (19) and d_e is de equivalent diameter.

$$Ra_e = \frac{\rho\, g\, \beta \left(T_i - T_o\right) d_e^{\,3}}{\nu^2} \, Pr \quad (19)$$

Equation (17) was found to be valid for $10^4 \leq Ra_i \leq 10^6$ and equation (18) was found to be valid for $10^5 \leq Ra_i \leq 10^6$.

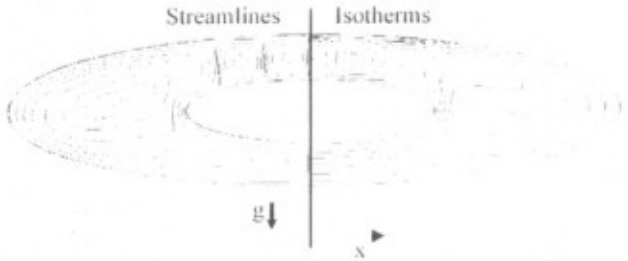

Figure 8 - Streamlines and isotherms for $b_o / a_o = 1/4$, $Per_i / Per_o = 0.4$ and Rayleigh number 10^5.

CONCLUSION

The analysis of the natural convection flow inside elliptical cavities allowed to appreciate the variety of flow patterns offered by these geometries. Of particular interest is the limiting case where Bénard cells are obtained, showing that for several perimeter ratios part of the elliptical cavity resembles the well-know flow between parallel plates heated from bellow. The remaining results can be incorporated to the others existing for complex geometries and be used for engineering calculations.

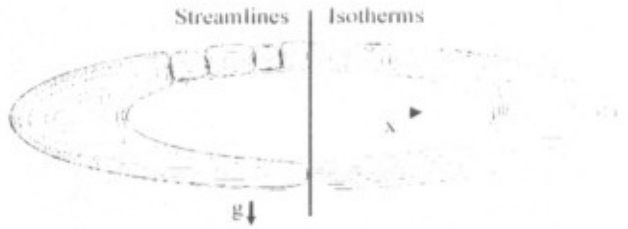

Figure 9 - Streamlines and isotherms for $b_o / a_o = 1/4$, $Per_i / Per_o = 0.6$ and Rayleigh number 10^5.

REFERENCES

Campo, E. M., Sen, M. and Ramos, E., 1987, *Natural Convection in a Semielliptic Cavity*, Numerical Heat Transfer, Vol. 12, pp. 101-119.

Kuehn, T. H. and Goldstein, R. J., 1978, *An Experimental Study of Natural Convection Heat Transfer in Concentric and Eccentric Horizontal Cylindrical Annuli*, Journal of Heat Transfer, Vol. 100, pp. 635-640.

Maliska, C. R., 1995, Transferência de Calor e Mecânica dos Fluidos Computacional - Fundamentos e Coordenadas Generalizadas, Livros Técnicos e Científicos Editora S/A (*in Portuguese*).

Marchi, C. H. and Maliska, C. R., 1994, *A Non orthogonal Finite-Volume Method for Solution of All Speed Flows using Co-Located Variables*, Numerical Heat Transfer - Part B, Vol. 26, pp. 293-311.

Raithby, G. D. and Torrence, K. E., 1974, *Upstream-Weighted Differencing Schemes and Their Application to Elliptic Problems Involving Fluid Flow*, Computers & Fluids, Vol. 2, pp. 191-206.

Peric, M., Kessler, R. and Scheuerer, G., 1988, *Comparison of Finite Volume Numerical Methods with Staggered and Co-located Grids*, Computers & Fluids, Vol. 16, pp. 389-403.

Schreiber, W. C. and Singh, S. N., 1987, *Natural Convection in a Stratified Fluid Between Confocal Horizontal Elliptical Cylinders*, Numerical Heat Transfer, Vol. 11, pp. 183-197.

Silva, A. F. C., Marchi, C. H., Livramento, M. A. and Azevedo, J. L. F., 1991, *On the Effects of Vectorization for Efficient Computation of three-dimensional Segregated Finite Volume Solutions*, Proceedings of the XI Brazilian Congress of Mechanical Engineering, pp. 109--112, São Paulo, Brazil.

Van Doormaal, J. P. and Raithby, G. D., 1984, *Enhancements of the SIMPLE Method for Predicting Incompressible Fluid Flow*, Numerical Heat Transfer, Vol. 7, pp. 147-163.

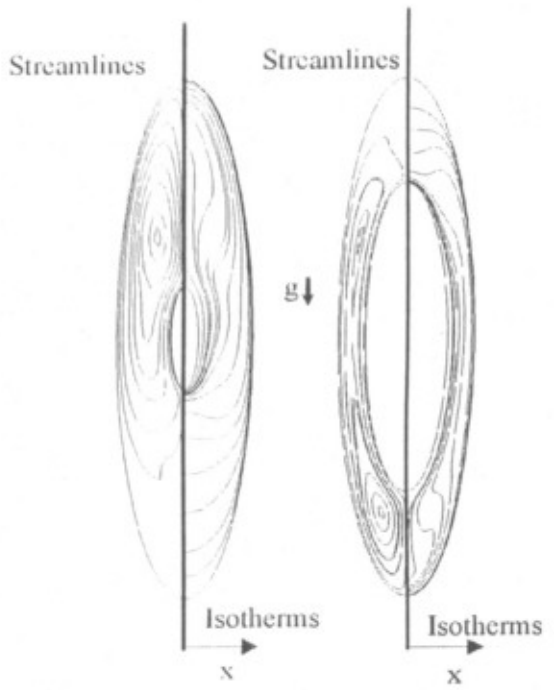

Figure 10 - Streamlines and isotherms for $b_o / a_o = 4/1$, $Per_i / Per_o = 0.2$ (left) and 0.6 (right) and Rayleigh number 10^5.

ACKNOWLEDGMENT

Financial support to A. R. Cunha and J. F. V. de Vasconcellos by Conselho Nacional de Desenvolvimento Cientifico e Tecnológico (CNPq) and to M. A. Livramento by Coordenação de Aperfeiçoamento do Pessoal de Ensino Superior (CAPES) are gratefully appreciated.